

# Thermal modeling CO<sub>2</sub> laser radiation transmission welding of superposed thermoplastic films

João M. P. Coelho

Manuel A. Abreu

Instituto Nacional de Engenharia e  
Tecnologia Industrial  
Optoelectronics Department  
Estrada do Paço do Lumiar 22  
1649-038 Lisboa, Portugal  
E-mail: jcoelho@dop.ineti.pt

F. Carvalho Rodrigues\*

Universidade Independente  
Faculdade de Ciências de Engenharia  
Avenue Marechal Gomes da Costa  
Lote 9  
1800-255 Lisboa, Portugal

**Abstract.** The low absorption presented by thermoplastic films to 10.6- $\mu\text{m}$  CO<sub>2</sub> laser radiation makes the engineering use of welding parameters, predicted by models developed for thicker thermoplastics, very difficult. A new theoretical model is developed describing the temperature distribution in thin thermoplastic material during the laser welding process. The heat conduction equation is solved analytically by the Green function method and heating and cooling thermal stresses are taken into consideration. Engineering parameters predicted by the model are applied to lap welding of high- and low-density polyethylene and polypropylene samples, both transparent and white, with thicknesses between 10 and 100  $\mu\text{m}$ , and experimentally validated. This validation is also accomplished by comparison with the measured temperature through the use of two diagnostic methods: schlieren interferometry and photothermal deflection spectroscopy. The first of these methods, combined with direct observation of Mie scattering, also puts in evidence the absorption of about 30% of the incident energy due to plasma formation in the air above the interaction interface. This plasma ignites after the initial release of chunks of material during the first moments of interaction. Proper modeling, and the introduction of a reflective substrate under the samples, allows an increase in process efficiency and the achievement of lap welding speeds up to 14  $\text{m s}^{-1}$  with this new transmission welding technique. © 2003 Society of Photo-Optical Instrumentation Engineers. [DOI: 10.1117/1.1615260]

Subject terms: lasers; transmission welding; thermoplastic films; modeling.

Paper 030076 received Feb. 11, 2003; revised manuscript received May 12, 2003; accepted for publication May 12, 2003.

## 1 Introduction

Laser devices, being versatile tools widely used in materials processing, have been subject to growing research in their application to the welding of thermoplastics. The demand of such consumer goods as food and medical products, to be packaged in plastic material in a way that quality and hygiene are preserved, has opened new areas in the laser application field.

The replacement of traditional tools, such as hot knives, ultrasound, or hot air, by laser tools can be justified by the increase in process reproducibility, simplicity of processing moving parts (no need for “stop and start” production lines), and productivity increase (the laser beam can scan the material faster than mechanical parts).<sup>1–6</sup> Also, being a noncontact and noncontaminating process, laser radiation was, from the start, an object of study for the thermoplastic industry.

According to Duley,<sup>5</sup> the first communications on plastic welding by laser appeared in the literature in 1972, reporting the welding of low-density polyethylene (LD PE) plates

with thicknesses on the order of a few millimeters, using 100-W power 10.6- $\mu\text{m}$  wavelength radiation emitted by a CO<sub>2</sub> laser and velocities of 10  $\text{mm s}^{-1}$ . However, it was in the last decade of the 20th century that research in this subject saw greater development, regarding increasing velocities,<sup>7,8</sup> new laser sources,<sup>9–11</sup> mathematical modeling,<sup>12–15</sup> and industrial applications.<sup>16–19</sup>

In 1992, Ou, Benatar, and Albright<sup>17</sup> presented the possibility of welding high-density polyethylene (HDPE) and polypropylene (PP) plates (6.3 mm thick) at 1.78  $\text{m min}^{-1}$  with a 2400-W CO<sub>2</sub> laser, while Duley and Mueller<sup>12</sup> referred to welding 1-mm PP at 4  $\text{cm s}^{-1}$  and 100-W laser power. In 1994, Jones and Taylor<sup>7</sup> welded PE at 1  $\text{m min}^{-1}$  with 100-W laser power, without, however, developing the appropriate process model. Also, Coelho, Abreu, and Pires<sup>8</sup> experimentally demonstrated in 2000 the viability of the laser lap welding of plastic films at up to 10  $\text{m s}^{-1}$ , with a 2700-W CO<sub>2</sub> laser.

Other work has been developed since 1998, in which the welding of superposed thermoplastics (lap welding) with different optical characteristics was studied.<sup>14,18,20–22</sup> This welding technique, known as transmission welding, uses two optically different thermoplastics: one transparent to laser radiation, the other highly absorbing. The opaque part

\*Current affiliation: NATO Headquarters, Division of Scientific and Environmental Affairs, B-1110, Brussels, Belgium.

**Table 1** Thermoplastics parameters for  $\lambda=10.6 \mu\text{m}$ .

	HD PE		LD PE transparent	PP transparent
	transparent	white		
Absorption coefficient $a_T$ [ $\times 10^3 \text{ m}^{-1}$ ], measured	0.822	1.561	1.092	3.831
Attenuation length $L$ [ $\times 10^{-3} \text{ m}$ ], measured	1.22	0.64	0.92	0.26
Complex refractive index, measured	$1.5-7 \times 10^{-4} i$	$1.5-10^{-3} i$	$1.6-9 \times 10^{-4} i$	$1.5-3 \times 10^{-3} i$
Thermal expansion coefficient $\alpha$ [ $\times 10^{-4} \text{ K}^{-1}$ ]	3.6	=	4.5	0.8
Thermal conductivity $K$ [ $\text{W m}^{-1} \text{ K}^{-1}$ ]	0.490	=	0.335	0.150
Density $\rho$ [ $\text{kg m}^{-3}$ ]	952	=	917	890
Specific heat capacity $C_p$ [ $\text{J kg}^{-1} \text{ K}^{-1}$ ]	3150	2737	1157	1469
Tensile modulus $E$ [ $\times 10^6 \text{ Pa}$ ]	0.80	=	0.25	1.35
Thermal diffusivity $k$ [ $\times 10^{-6} \text{ m}^2 \text{ s}^{-1}$ ]	0.16	0.19	0.32	0.12
Melting temperature $T_f$ [K], measured	396	=	377	433
Welding temperature $T_s$ [K]	474	=	474	500
Latent heat of fusion $L_f$ [ $\text{J kg}^{-1}$ ]	103340	91685	34120	47005

absorbs the radiation and heats the transparent part by heat conduction.

All the work presented by these authors considers total absorption by at least one of the parts. However, most thermoplastics used in the packaging industry, like HD PE, LD PE, and PP, with thicknesses lower than  $100 \mu\text{m}$ , have low absorption to laser radiation, typically lower than 20%, presenting in most cases an attenuation length, defined as the inverse of the absorption coefficient  $a_T$ , higher than their thickness, as shown by Coelho et al.<sup>23</sup>

In this work, a model is developed that allows the lap welding parameters of transparent HD and LD PE, PP and white HD PE samples to be obtained, all with thickness  $h$  lower than  $100 \mu\text{m}$ , in a situation of transmission welding without a total absorbing part. Table 1 shows the relevant physical parameters of the thermoplastics considered.

## 2 Thermodynamic Model

Since welding thermoplastics using  $10.6\text{-}\mu\text{m}$  laser radiation involves thermodynamic phenomena, it is important to define a model based on the heat transfer that occurs during the process.

The quantity that is conserved, generated, or lost in the theory of heat conduction is thermal energy. Its density per unit mass of a material (solid or liquid) of density  $\rho$  [ $\text{kg m}^{-3}$ ] and specific heat at constant pressure  $C_p$  [ $\text{J kg}^{-1} \text{ K}^{-1}$ ] is given by  $\rho \int C_p dT$ , and the rate of heat transfer vector is given by  $\vec{Q} = -K \cdot \nabla T + \rho \vec{v} \int C_p dT$ , where  $K$  [ $\text{W m}^{-1} \text{ K}^{-1}$ ] is the thermal conductivity, and  $\vec{v}$  the velocity vector. If the temperature change in time and a heat source is present, then the following energy balance can be made:

Energy  
conducted to  
the inside of  
the material

+

Interior  
generated heat

=

Energy conducted  
to the outside of the  
material

+

Change of  
internal  
energy

and the heat conduction equation is then<sup>24,25</sup>

$$\left\{ \frac{\partial \rho}{\partial t} + \nabla \cdot (\rho \vec{v}) \right\} \int C_p dT + \rho C_p \left( \frac{\partial T}{\partial t} + \vec{v} \cdot \nabla T \right) = \nabla \cdot K \nabla T + Q(r). \quad (1)$$

Due to mass conservation, this equation simplifies to

$$\rho C_p \left( \frac{\partial T}{\partial t} + \vec{v} \cdot \nabla T \right) = \nabla \cdot K \nabla T + Q(r). \quad (2)$$

Considering  $K=K(T)$ , defining the thermal diffusivity  $k$  [ $\text{m}^2 \text{ s}^{-1}$ ] as

$$k = \frac{K}{\rho C_p},$$

and with  $\rho$ ,  $C_p$ , and  $k \sim$  constants, Eq. (2) becomes

$$\frac{\partial T}{\partial t} + \vec{v} \cdot \nabla T = k \nabla^2 T + \frac{Q(r)}{\rho C_p}. \quad (3)$$

If, as assumed in this work, the thermoplastic to be welded moves in one direction only (say,  $XX$ ), then Eq. (3) can take the form

$$\begin{aligned} \frac{\partial}{\partial t} \{ \Delta T(r, t) \} &= k \nabla^2 \{ \Delta T(r, t) \} - v_x \frac{\partial}{\partial x} \{ \Delta T(r, t) \} \\ &+ \frac{1}{\rho C_p} Q(r), \end{aligned} \quad (4)$$

where  $\Delta T(r, t)$  is the temperature change (to ambient temperature) and  $r$  represents the  $x$ ,  $y$ , and  $z$  coordinates. The heat produced by the material due to the absorption of laser radiation is given by

$$\begin{aligned} Q(r) &= a_T \cdot I(r) \cdot \exp(-a_T \cdot z) \\ &= \frac{4a_T P}{\pi \left(\frac{d}{2}\right)^2} \exp\left[-\frac{2(x^2 + y^2)}{\left(\frac{d}{2}\right)^2}\right] \cdot \exp(-a_T \cdot z), \end{aligned} \quad (5)$$

where  $P$  [W] represents the average power delivered by the laser and  $d$  [m] is the beam diameter on the material.

For the case of thermoplastic films processed at velocities higher than  $1 \text{ m s}^{-1}$ , the medium can be considered as an infinite half space, since  $h \gg 2k/v_x$  is valid<sup>24</sup> (as can be seen in Table 1). Then, considering the laser beam propagating in the  $ZZ$  direction, the boundary conditions to solve Eq. (4) are

$$\begin{aligned} \Delta T(x, y, z, t) \Big|_{t=0} &= 0, \\ \Delta T(x, y, z, t) \Big|_{x, y, z = \pm \infty} &= 0, \\ \delta T(x, y, z, t) \Big|_{t=0} &= 0, \end{aligned} \quad (6)$$

with  $\delta T$  being the temperature gradient.

Then, using the Green function,<sup>26–29</sup> the solution can be written as

$$\begin{aligned} \Delta T(x, y, z, t) &= \int_{-\infty}^{+\infty} \int_{-\infty}^{+\infty} \int_0^{+\infty} \int_0^{+\infty} Q(\xi, \eta, \mu, \tau) \\ &\cdot G\left(\frac{x}{\xi}, \frac{y}{\eta}, \frac{z}{\mu}, \frac{t}{\tau}\right) \cdot d\xi \cdot d\eta \cdot d\mu \cdot d\tau. \end{aligned} \quad (7)$$

This methodology has the advantage that the Green function is independent of the nonhomogeneous terms of the differential equation; then, having determined the Green function, the solution can be obtained by simple integration.<sup>30</sup> The Green function satisfies the differential equation

$$\begin{aligned} \frac{\partial G}{\partial t} - k \nabla^2 G + v_x \frac{\partial G}{\partial x} &= \frac{1}{\rho C_p} \delta(x - \xi) \delta(y - \eta) \delta(z - \mu) \\ &\times \delta(t - \tau), \end{aligned} \quad (8)$$

where  $\delta$  represents Dirac's delta function. Applying the Fourier transform, the solution of Eq. (8) in the space  $\omega_x$ ,  $\omega_y$ , and  $\omega_z$  is

$$\begin{aligned} \frac{\partial G_F}{\partial t} + k(\omega_x^2 + \omega_y^2 + \omega_z^2) G_F - i\omega_x v_x G_F \\ = \frac{1}{(2\pi)^{3/2} \rho C_p} \exp[i(\omega_x \xi + \omega_y \eta + \omega_z \mu)] \delta(t - \tau), \end{aligned} \quad (9)$$

where  $G_F$  represents the Fourier transform of  $G$ . To simplify Eq. (9), the Laplace transform is applied, obtaining

$$\begin{aligned} s G_{FL} + k(\omega_x^2 + \omega_y^2 + \omega_z^2) G_{FL} - i\omega_x v_x G_{FL} \\ = \frac{1}{(2\pi)^{3/2} \rho C_p} \exp[i(\omega_x \xi + \omega_y \eta + \omega_z \mu)] \exp(-s\tau), \end{aligned} \quad (10)$$

or

$$G_{FL} = \frac{1}{(2\pi)^{3/2} \rho C_p} \cdot \frac{\exp[i(\omega_x \xi + \omega_y \eta + \omega_z \mu)] \exp(-s\tau)}{s + k \cdot (\omega_x^2 + \omega_y^2 + \omega_z^2) - i\omega_x v_x}, \quad (11)$$

where  $G_{FL}$  is the Laplace transform of  $G_F$ . Inverting these operations allows the Green function to be obtained as

$$\begin{aligned} G &= \frac{u(t - \tau)}{[4\pi k(t - \tau)]^{3/2} \rho C_p} \\ &\cdot \exp\left\{-\frac{[x - \xi + v_x(t - \tau)]^2 + (y - \eta)^2 + (z - \mu)^2}{4k(t - \tau)}\right\}. \end{aligned} \quad (12)$$

Then, introducing Eqs. (12) and (5) into Eq. (7) results in

$$\begin{aligned} \Delta T(x, y, z, t) &= \frac{2a_T \cdot P}{\pi \rho C_p} \cdot \int_0^t \frac{1}{\left(\frac{d}{2}\right)^2 + 8k(t - \tau)} \\ &\times \exp\left\{-\frac{[x - v_x(t - \tau)]^2 + y^2}{\left(\frac{d}{2}\right)^2 + 8k(t - \tau)}\right\} \\ &\times \{a_T [k(t - \tau) - z]\} \\ &\cdot \text{erfc}\left\{\frac{2a_T \cdot k(t - \tau) - z}{[4k(t - \tau)]^{1/2}}\right\} \cdot d\tau. \end{aligned} \quad (13)$$

However, as previously stated, the thermoplastic films that are the subject of this work present high transmission to the laser radiation, and the heat conduction in the material is reduced due to low thermal conductivity values. So, the influence of  $z$  can be disregarded from the solution, except for the term  $\exp(-a_T z)$  for considering beam attenuation through the path. Then, the model can become

$$\Delta T(x, y, z, t) = \frac{4a_T \cdot P}{\pi \rho C_p} \exp(-a_T \cdot z) \cdot \int_0^t \frac{1}{\left(\frac{d}{2}\right)^2 + 8k(t-\tau)} \times \exp\left\{-\frac{[x-v_x(t-\tau)]^2 + y^2}{\left(\frac{d}{2}\right)^2 + 8k(t-\tau)}\right\} d\tau. \quad (14)$$

The thermal behavior while cooling can be predicted by the relation

$$\Delta T(x, y, z, t)|_{t > t_{\text{inter}}} = \Delta T(x, y, z, t) - \Delta T(x, y, z, t - t_{\text{inter}}), \quad (15)$$

where  $t_{\text{inter}}$  is the interaction time.

Also, due to the high transparency that thermoplastic films present to 10.6- $\mu\text{m}$  laser radiation, the introduction of a reflective material under the superposed films—a metallic substrate—was considered. This presence can be simulated by considering the existence of another source under the thermoplastic, resulting from reflectance  $R^*$ , and is expected to improve process efficiency. Then Eq. (14) should be altered accordingly, resulting in:

$$\Delta T(x, y, z, t) = \Delta T(x, y, z, t)|_{\bar{w}/\text{subst}} + (1-A)^2 \cdot R^* \cdot \Delta T(x, y, |z-2 \cdot h|, t)|_{\bar{w}/\text{subst}}, \quad (16)$$

representing  $\Delta T(x, y, z, t)|_{\bar{w}/\text{subst}}$ , the value expected without the substrate, given by Eq. (14) or (15), and  $A$ , the film's absorptance.

The previous relations allow the prediction of the engineering parameters needed to achieve a temperature that, for welding purposes, is the welding temperature  $T_s$ . It is common methodology to consider the delivered energy density  $(E/A_r)_0$  as a useful parameter, combining the values of the process variables: laser incident power  $P_0$ , displacement velocity  $v_x$ , and laser spot diameter  $d$ , over the material. Then the equation

$$\left(\frac{E}{A_r}\right)_0 = \frac{4P_0}{\pi \cdot v_x \cdot d}, \quad (17)$$

relates all the most important engineering parameters involved in laser processing. However, besides the energy density needed to increase the thermoplastic temperature to an appropriate level, it is also necessary to consider the thermal stresses that occur during the interaction.<sup>12,31</sup>

The expression that gives the material's expansion (or contraction)  $\Delta L$  of the linear dimension  $L$  of a material with linear thermal expansion coefficient  $\alpha_L [K^{-1}]$  subjected to a temperature change  $\Delta T$  is<sup>31,32</sup>

$$\Delta L = \alpha_L \cdot L \cdot \Delta T. \quad (18)$$

This expression describes the expansion during the heating phase and the contraction during cooling. If one considers that the temperature distribution is symmetric with respect to its maximum, then as the material cools, opposite compressive forces appear in the  $YY$  direction. This allows

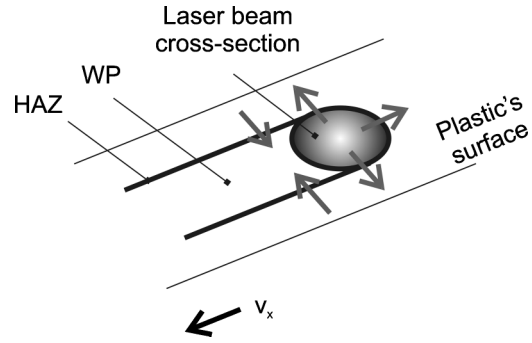


Fig. 1 Simplified schematic representing the action of thermal stresses (arrows) while processing. WP is the weld pool and HAZ is the heat affected zone.

the mixture and distribution of the molten material. Figure 1 shows a simplified schematic of this phenomenon. So, to achieve welding between the two superposed plastic films, the laser beam cross section over the thermoplastics must have a diameter that allows the proper mixture and distribution of the molten material. This value can be predicted, assuming that the minimum beam diameter  $d_0$  should be at least of the same magnitude as the film's thickness. Then, from Eq. (18) the condition is

$$d_0 > 2 \cdot h \cdot \alpha_L \cdot \Delta T, \quad (19)$$

with  $\Delta T = T_s - T_0$ , and  $T_0$  being the environment temperature.

### 3 Experimental Procedures for Verification of the Theoretical Predictions

The thermodynamic model defined in Sec. 2 allowed the prediction of the engineering parameters necessary to obtain welding between superposed thermoplastic films with thicknesses lower than 100  $\mu\text{m}$ . These parameters were applied using two experimental configurations: 1. for welding trials at velocities lower than 1  $\text{m s}^{-1}$ , we used a 400-W Léctra Systèmes fast axial flux CO<sub>2</sub> laser and an X-Y translation table; 2. for higher velocity tests, we used a 140-2700-W Trumpf CO<sub>2</sub> fast axial flux laser and a rotating drum. A schematic of this last setup is shown in Fig. 2, where the thermoplastic samples are placed around the drum's curved surface. High linear velocities of up to 20  $\text{m s}^{-1}$  were reached by the plastic samples. In both configurations, the focusing lens (with focal length  $f = 120$  and 50 mm, respectively) could change its position with relation to the samples. This focus offset  $\Delta$  allows high beam diameters to be obtained over the sample's surface.

Under the samples, an aluminum substrate was used to maximize the process efficiency. Its reflectance was measured  $R^* = 63\%$ , and no significant diffusion was observed on the reflected beam.

After submitting the samples to laser interaction, the lap weld strength was tested in a tensile system. Each sample was divided into several specimens, each 60 mm long by 40 mm wide. Then, a uniform load was applied perpendicular to the weld seam, and increased (at about 9  $\text{N s}^{-1}$ ) until rupture. The value of tensile strength  $S$  for each weld was compared to that of the original thermoplastic and results

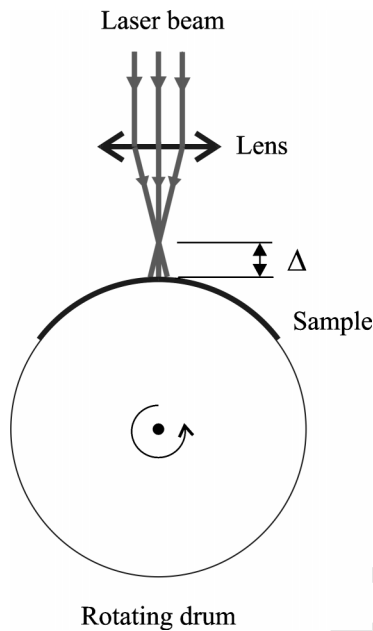


Fig. 2 Schematic of the experimental setup used for high-velocity welding.

were plotted as a percentage of the latter. The manufacturers' data considered that a "good weld" occurs when  $S > 80\%$ .<sup>33</sup>

Also, two diagnostic and measurement methods were used to obtain the thermoplastic processing temperature: schlieren interferometry<sup>36</sup> and photothermal deflection spectroscopy (PTDS).<sup>37,38</sup> The schlieren interferometry diagnostic method, whose schematic is shown in Fig. 3, uses a visible probe beam, filtered and expanded, which passes through the area above the interaction zone before being focused on a shear plate and projected onto a target. A CCD camera records the resulting pattern, and its analysis allows the temperature distribution on the thermoplastic/air interface to be obtained. The PTDS method just analyzes the deflection of the probe beam as it passes through the region. In both cases, the temperature at the thermoplastic surface can be determined by applying a proper heat transfer solution.<sup>26</sup>

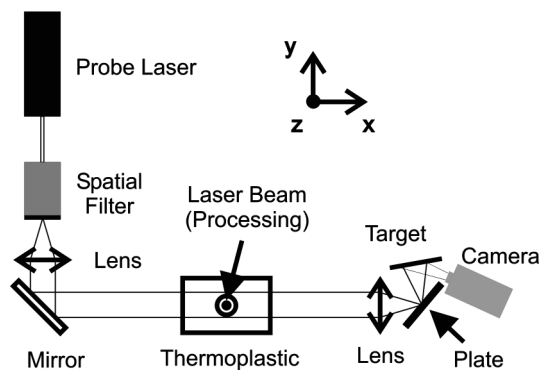


Fig. 3 Schlieren interferometry setup schematic.

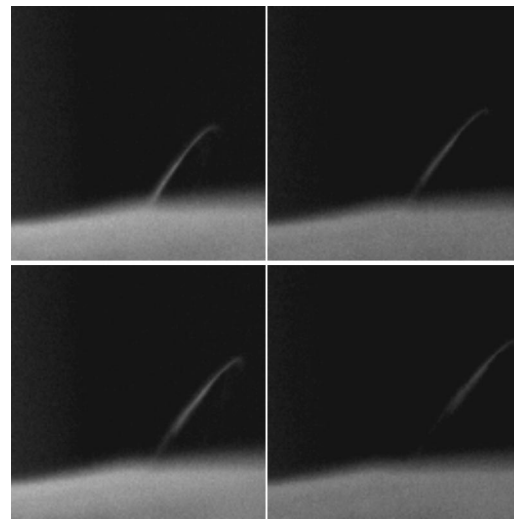


Fig. 4 Example of a sequence of material release while processing, filmed with a 100-Hz CCD camera.

#### 4 Results and Discussions

The application of practical parameters from Eq. (16), obtained for welding temperature  $T_s$ , has shown that 30% more than the predicted plus of delivered energy is necessary to obtain welding. This phenomenon could have arisen for several reasons. One is the existence of changes in the expected beam diameter; however, this was not observed. Another possibility is the absorption of the 10.6- $\mu\text{m}$  laser radiation by the medium (air); however, the equivalent attenuation coefficient is too small (lower than  $0.2 \times 10^{-3} \text{ m}^{-1}$ ) to have significant influence.

The hypothesis considered was the absorption of laser radiation by products released during the initial moments of processing, setting up conditions for the formation of a plasma above the plastic's surface. This hypothesis was proven by Mie scattering, direct observation, and schlieren interferometry.

Figure 4 shows an example of material released during the  $0.042 \text{ m s}^{-1}$  processing of a 10- $\mu\text{m}$  transparent HD PE, observed through a high-speed CCD camera (100-Hz acquisition rate). Figure 5 shows an example of plasma formation under the same conditions, and Fig. 6 shows the scattering of a 633-nm He-Ne laser radiation probe beam as it passes through the interaction interface.

Work developed on gaseous emission during CO<sub>2</sub> laser processing of thermoplastics<sup>39,40</sup> indicates that the main products are aerosols, between  $140 \text{ mg m}^{-3}$  and more than  $300 \text{ mg m}^{-3}$ . According to Haferkamp et al.,<sup>39</sup> polyolefines like PE and PP have more than 70% of the particles generated in the range 0.13 to 0.50  $\mu\text{m}$ , thus contributing to the event of Mie scattering. This information was assumed as qualitative information. Further work should be developed to quantify the specificity of each situation.

The application of a schlieren interferometer allowed the temperature distribution above the thermoplastic's surface to be obtained and to confirm that the heat exchange by convection between the plasma and the air is about 30% of the delivered energy, thus validating the former hypothesis.<sup>35</sup>

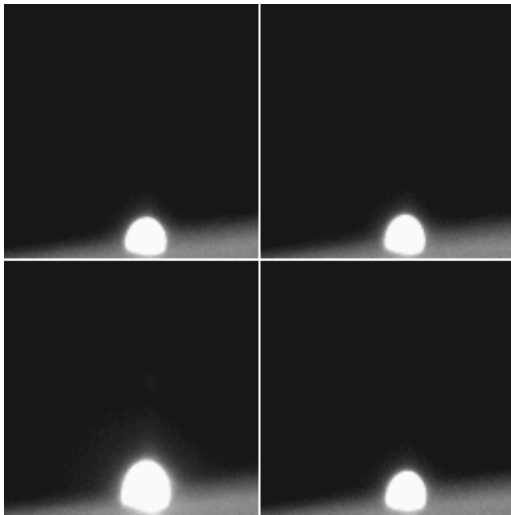


**Fig. 5** Example of a plasma formation sequence while processing, filmed with a 100-Hz CCD camera.

The plasma, only visible using the CCD camera with exposure times lower than 500  $\mu\text{s}$ , is expected to have reduced dimensions and to be positioned above the thermoplastic/air interface.

In spite of a continuous absorption of 30% of the incident energy, the plasma is only visible when critical densities of vaporized material are achieved. The plasma plume is created above the sample surface, and radiates energy over a large spectrum bandwidth and in all directions. Presumably, only a small portion of this energy reaches the sample. This may explain why the event of a plasma with temperatures higher than 3000 K have no visible effect on the thermoplastic interface.

The effect of this phenomenon in the weld seam dimensions can be deduced from the data plotted in Fig. 7. The evolution of weld seam diameter  $W_s$  as the energy density applied increases (welding of 30- $\mu\text{m}$  transparent HD PE samples) is plotted, and allows comparison of the situations with and without fume removal. Based on this graph, it is clear that the material released also affects the weld seam dimensions. The reduction that is observed might be due to the interaction between the plasma that was created and the laser beam.

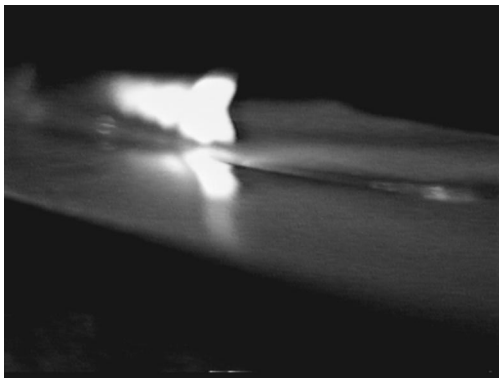


**Fig. 6** Example of Mie scattering, filmed by a 100-Hz CCD camera.

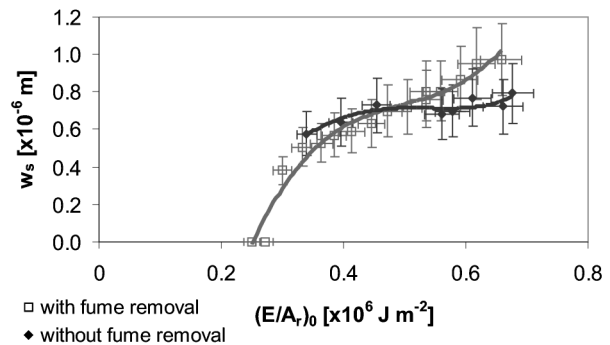


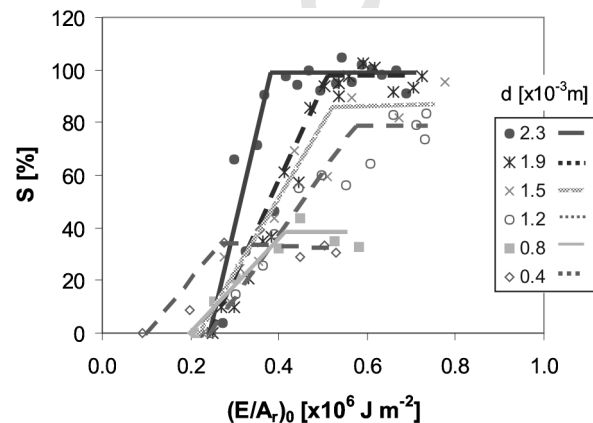
**Fig. 7** Influence of applied energy density  $(E/A_r)_0$  on measured weld seam diameter  $w_s$  for 30- $\mu\text{m}$  transparent HD PE, with and without fume removal.

Based on these observations, the values of  $P_0$  (or  $E/A_r$ ) predicted by the model should be adjusted by a term  $(1+\beta)$  to be applied in welding procedures,  $\beta$  being the power loss before reaching the sample surface; in our case,  $\beta=0.3$ . Removing any interaction product by applying a gas jet parallel to the surface makes  $\beta\sim 0$ .

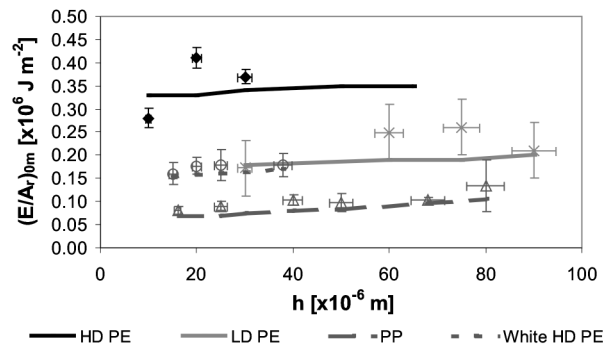
From the condition in Eq. (18), and assuming the material parameters in Table 1,<sup>41–44</sup> it is predicted that  $d_0 > 1.2$  mm. Figure 8 shows an example of weld strength behavior as  $(E/A_r)_0$  increases for different values of  $d$  (2  $\text{m s}^{-1}$  processing of a 30- $\mu\text{m}$  transparent HD PE). It can be seen that, as expected, only for values higher than 1.2 mm is welding achieved.

Figure 9 shows the comparison between predicted (lines) and experimental (points) with  $(E/A_r)_0$  minimum values for welding all the thermoplastic films considered. Predicted values have a standard deviation of 12% (not shown on the graph) and the presence of a reflective aluminum substrate under the samples is assumed. These values were constant (within their standard deviation) with processing velocity.

Comparing the theory with the values measured using schlieren spectroscopy, and PTDS, validated the temperature model. Figure 10 shows an example of plotting the predicted and measured temperatures for the processing of



**Fig. 8** Influence of beam spot diameter  $d$  on weld strength  $S$  for 30- $\mu\text{m}$  transparent HD PE, and  $v_x=2$   $\text{m s}^{-1}$ .



**Fig. 9** Comparison between predicted (lines) and experimental (points) welding minimum energy density delivered to the samples  $(E/A_r)_{0m}$ .

a 30- $\mu\text{m}$  transparent HD PE with 44-W laser power,  $v_x = 0.042 \text{ m s}^{-1}$  and  $d = 1.6 \text{ mm}$ .

Table 2 summarizes all the engineering parameters obtained. It shows the minimum energy density  $(E/A_r)_{0m}$  delivered to the sample, the minimum weld strength  $S$ , the minimum beam diameter  $d_0$ , and the maximum processing velocity  $v_{max}$ , achieved. It can be observed that welding was accomplished for the majority of the thermoplastics, with the exception of those with 10 and 15  $\mu\text{m}$  thicknesses. This seems to occur due to the dynamic presented during the processing of these thinner samples: the expansive forces do not allow the mixture of the molten material from the two superposed films. The image sequence presented in Fig. 11, obtained with a 25-Hz CCD camera, reveals this phenomenon.

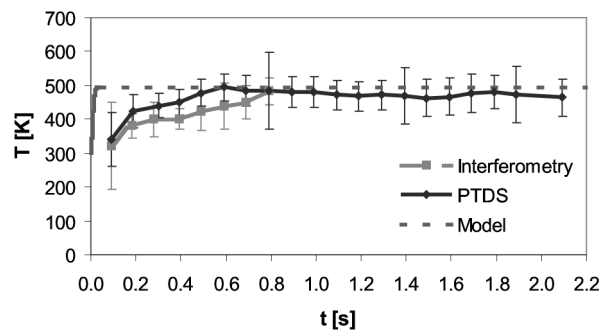


**Fig. 10** Surface temperature variation with processing time as predicted by thermal model and measured by schlieren interferometry and PTDS. (Transparent 30- $\mu\text{m}$  HD PE,  $P = 44 \text{ W}$ ,  $v_x = 0.042 \text{ m s}^{-1}$ , and  $d = 1.6 \text{ mm}$ .)

From Table 2, it can also be seen that welding was accomplished at velocities higher than  $2 \text{ m s}^{-1}$ , and even at  $14 \text{ m s}^{-1}$ , which is a major improvement on the reported state of the art processing velocities. The introduction of a reflective substrate under the thermoplastics samples is mainly responsible for this success, which allowed a reduction of between 30 and 40% of the necessary energy density.

## 5 Conclusions

The validity of a simple model illustrating the process of laser lap welding of 10- to 100- $\mu\text{m}$  thermoplastic films is demonstrated. The approach, based on the Green function method, allows successful prediction of the temperature distribution in the material to optimize the welding param-

**Table 2** Summary of experimental engineering parameters achieved for lap welding of thermoplastic films.

Thermoplastic	$h$ [ $\times 10^{-6} \text{ m}$ ]		$(E/A_r)_{0m}$ [ $\times 10^6 \text{ J m}^{-2}$ ]	$v_{max}$ [ $\text{m s}^{-1}$ ]
Transparent LD PE	30	$S > 80\% @ d_0 = 1.2 \text{ mm}$	0.17	7
	60	$S > 80\% @ d_0 = 2.3 \text{ mm}$	0.25	2
	75	$S > 80\% @ d_0 = 1.9 \text{ mm}$	0.30	2
	90	$S > 80\% @ d_0 = 1.2 \text{ mm}$	0.21	2
	120	$S > 80\% @ d_0 = 1.2 \text{ mm}$	0.27	10
Transparent HD PE	10	$S = 54\% @ d_0 = 1.9 \text{ mm}$	0.27	2
	20	$S > 80\% @ d_0 = 1.9 \text{ mm}$	0.41	4
	30	$S > 80\% @ d_0 = 1.2 \text{ mm}$	0.37	6
White HD PE	15	$S = 61\% @ d_0 = 1.9 \text{ mm}$	0.17	5
	20	$S > 80\% @ d_0 = 1.9 \text{ mm}$	0.18	2
	25	$S > 80\% @ d_0 = 1.2 \text{ mm}$	0.18	10
	38	$S > 80\% @ d_0 = 1.2 \text{ mm}$	0.18	14
Transparent PP	16	$S > 80\% @ d_0 = 2.3 \text{ mm}$	0.08	3
	25	$S > 80\% @ d_0 = 1.2 \text{ mm}$	0.09	10
	40	$S > 80\% @ d_0 = 1.2 \text{ mm}$	0.10	7
	50	$S > 80\% @ d_0 = 1.2 \text{ mm}$	0.10	14
	68	$S > 80\% @ d_0 = 1.9 \text{ mm}$	0.10	14
	80	$S > 80\% @ d_0 = 1.2 \text{ mm}$	0.14	10

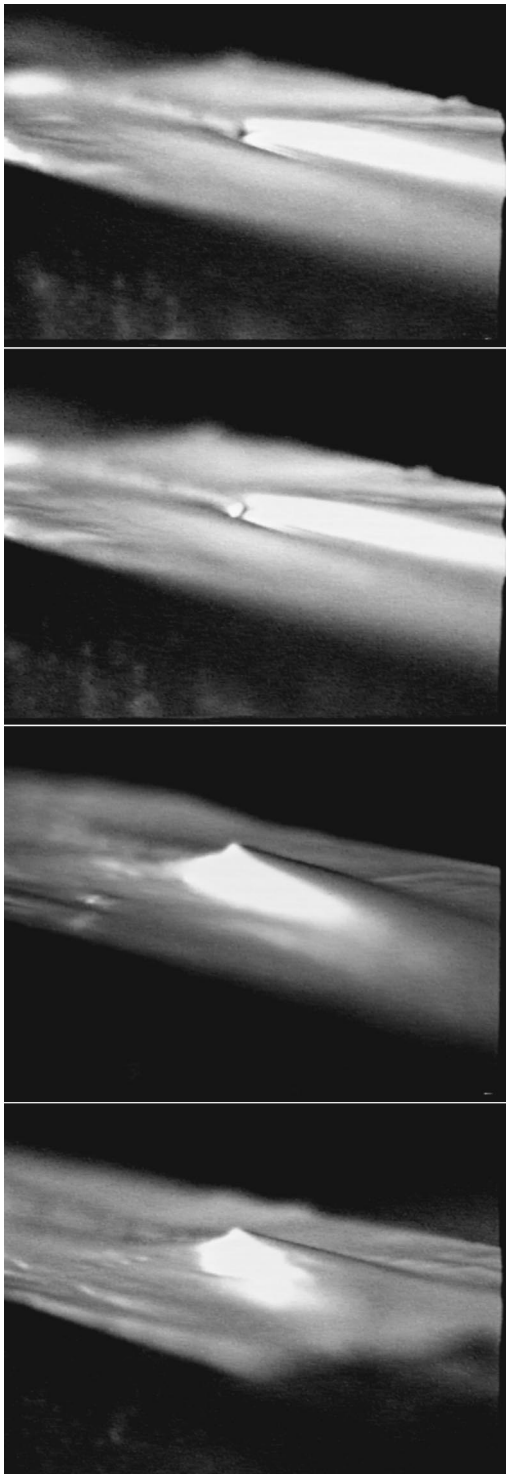


**Fig. 11** Sequence showing the surface dynamics when processing a 10- $\mu\text{m}$  HD PE, filmed with a 25-Hz CCD camera.

eters. Using two diagnostic methods—schlieren interferometry and photothermal spectroscopy—a better understanding of all related physical phenomena is made possible. These theoretical and experimental procedures allow welding (weld tensile strength higher than 80%) transparent HD PE at up to  $6\text{ m s}^{-1}$ , LD PE at up to  $10\text{ m s}^{-1}$ , and white HD PE and transparent PP at up to  $14\text{ m s}^{-1}$ , with a 2.7-kW

CO<sub>2</sub> laser and a 1.2-mm-diam beam. Further work should be developed to overcome the difficulties encountered in lap welding of 10 and 15  $\mu\text{m}$  HD PE films. However, this work demonstrates the viability of high-speed transmission welding of superposed thermoplastic films that have attenuation lengths greater than their thickness.

### Acknowledgments

The authors wish to thank the NATO Science for Stability Program for funding part of this work. The authors also wish to thank their colleagues Margarida Pires, Jerónimo Silva, Fernando Monteiro, and José Manuel Rabaça for their collaboration in this work, and José Cabrita Freitas for his support.

### References

1. Kamweld Technologies, "How plastics welding progressed," see [http://www.kamweld.com/html/how\\_plastic\\_welding\\_progressed.html](http://www.kamweld.com/html/how_plastic_welding_progressed.html).
2. TWI, "Weldability of thermoplastics," see [http://www.twi.co.uk/j32k/protected/band\\_3/ksfc003.html](http://www.twi.co.uk/j32k/protected/band_3/ksfc003.html).
3. "Welding developments," PRW Ancillaries, 10 Nov., 1995.
4. J. D. Gaspar, "Better bonds: Plastics welding gets smarter, faster, stronger," *Plast. Technol.* ■, 42–45 (1996).
5. W. W. Duley, *Laser Welding*, pp. 143–144, John Wiley and Sons, New York (1999).
6. V. A. Kagan, "Innovations in laser welding of thermoplastics: This advanced technology is ready to be commercialized," *Soc. Automotive Engineers, Inc.* (2002).
7. I. A. Jones and N. S. Taylor, "High speed welding of plastics using lasers," *ANTEC '94*, pp. 1360–1363 (1994).
8. J. P. Coelho, M. A. Abreu, and M. C. Pires, "High-speed laser welding of films," *Opt. Lasers Eng.* **34**, 385–395 (2000).
9. "Laser diode welder joins plastic parts," *Europhotonics*, pp. 14–15 (1997).
10. "Infrared welding joins rubber, foam and reinforced polymers," *Opto Laser Europe*, pp. 17 (1999).
11. J. Schultz and E. Habberstroh, "Welding of polymers using a diode laser," in *Proc. 58th Annual Conf. Exhibits*, Society of Plastic Engineers, pp. 1196–1201 (2000).
12. W. Duley and R. Mueller, "CO<sub>2</sub> laser welding of polymers," *Polym. Eng. Sci.* **32**(9), 582–585 (1992).
13. P. A. Atanasov, "Laser welding of plastics: Theory and experiments," *Opt. Eng.* **34**(10), 2974–2980 (1995).
14. H. Potente, J. Korte, and F. Becker, "Laser transmission welding of thermoplastics: Analysis of the heating phase," *ANTEC '98*, pp. 1022–1025 (1998).
15. D. Schuoecker and A. Kaplan, "Overview of modeling for laser applications," *Proc. SPIE* **2207**, 236–247 (1994).
16. "Laser welding in high-speed option for film fabricators," *Mod. Plastics Intl.*, pp. 30–32 (1994).
17. B. S. Ou, A. Benatar, and C. W. Albright, "Laser welding of polyethylene and polypropylene plates," *Soc. Plastics Eng. ANTEC '92*, pp. 1764–1767 (1992).
18. EWI, "Trough-transmission Infrared Welding TTIR," see <http://www.ewi.org/ewi/ttir.html>.
19. H. Haferkamp, A. von Busse, O. Thurk, and M. Goede, "Welding of automotive polymeric components using laser radiation," *Proc. Auto. Transport. Technol.* **3**, 7 pages (2001).
20. Fraunhofer USA, "Laser welding of plastics," see <http://www.frcmi.fraunhofer.com/laser/projects/plasticwelding.html>.
21. R. Leaversuch, "Laser welding comes of age," *Plastics Technol. Online* (2002).
22. P. A. Hilton, I. A. Jones, and Y. Kennish, "Transmission laser welding of plastics," *Proc. SPIE* **4831**, 44–52 (2003).
23. J. M. P. Coelho, P. M. R. Sampaio, and M. C. Pires, "Thin plastic films optical parameters for CO<sub>2</sub> and Nd:YAG lasers radiation," *Proc. Int. Conf. Lasers '98*, pp. 516–519, STS Press (1999).
24. J. M. Dowden, *The Mathematics of Thermal Modeling: An Introduction to the Theory of Laser Material Processing*, pp. 20–30, Chapman & Hall, Boca Raton, FL (2001).
25. W. M. Steen, *Laser Material Processing*, pp. 145–149, Springer-Verlag, London (1991).
26. B. A. Boley and J. H. Weiner, *Theory of Thermal Stresses*, pp. 152, 179–183, John Wiley and Sons, New York (1960).
27. M. von Allmen, *Laser-Beam Interactions with Materials: Physical Principles and Applications*, pp. 206–208, Springer-Verlag, Berlin Heidelberg (1987).

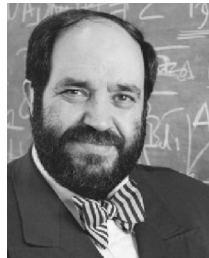
28. S. A. Pahl, "Charts to rapidly estimate temperature following laser irradiation," *Proc. SPIE* **2391**, 499–511 (1995).
29. J. C. Conde, F. Lusquinos, P. González, B. León, and M. Pérez-Amor, "Temperature distribution in laser marking," *J. Laser Appl.* **3**(3), 105–110 (2001).
30. B. di Prima, *Elementary Differential Equations and Boundary Value Problems*, pp. 509, John Wiley and Sons, New York (1969).
31. D. Porter, *Group Modelling of Polymer Properties*, Marcel Dekker, Inc., New York (1995).
32. Donnelly Bros. Inc., The Online Materials Information Resource, see <http://www.matweb.com>.
33. "Thermal and chemical welding of plastics materials," in *Engineering Equipment Users Association Handbook* **35**, pp. 7–9 (1976).
34. F. Carvalho Rodrigues, J. Coelho, and M. Abreu, "Aplicação da interferometria de schlieren e da espectroscopia de deflexão fototérmica à medição da temperatura durante o processamento por laser," *Proc. 13<sup>a</sup> Conf. Nac. de Física—Física 2002*, pp. 487–489, Sociedade Portuguesa de Física (2002).
35. J. M. P. Coelho, M. A. Abreu, and F. Carvalho Rodrigues, "Application of schlieren interferometry to temperature measurements during laser welding of high-density polyethylene films," (submitted for publication).
36. M. R. Barrault, G. R. Jones, and F. Carvalho Rodrigues, "Practical arcing environments arc plasma diagnostics," *Proc. 7th Yugoslav Symp. Summer School Physics Ionized Gases*, pp. 701–807 (1974).
37. S. E. Bialkowski, *Photothermal Spectroscopy Methods for Chemical Analysis*, pp. 1–39, John Wiley and Sons Inc., New York (1996).
38. W. B. Jackson, N. M. Amer, A. C. Boccara, and D. Fournier, "Photothermal deflection spectroscopy and detection," *Appl. Opt.* **20**(8), 1333–1344 (1981).
39. H. Haferkamp, M. Goede, K. Engel, and J. S. Wittbecker, "Hazardous emissions: characterization of CO<sub>2</sub> laser material processing," *J. Laser Appl.* **■**, 83–88 (1995).
40. M. Botts, "New data help industry to meet safety directives," *Opto Laser Europe*, pp. 33–34 (1995).
41. Donnelly Bros. Inc., MathWeb—The Online Materials Information Resource, see <http://www.mathweb.com>.
42. J. H. Perry and D. Green, *Chemical Engineers' Handbook*, McGraw-Hill, New York (1983).
43. P. C. Powell, *Plastics*, Kempe's Engineers Yearbook 90th ed., pp. C2–15, Publishing Co. Ltd., London (1985).
44. Plasticusa Reports, "Plastic material properties," see <http://www.plasticusa.com/>.



**João M. P. Coelho** received his engineering degree in physics and materials engineering in 1992 from UNL, Lisbon, Portugal. He is a researcher in the optoelectronics department of the Instituto Nacional de Engenharia e Tecnologia Industrial (INETI), in Lisbon, and is currently pursuing a PhD degree in physics engineering at the Technical University of Lisbon. His research interests include laser material processing, optical systems design, and remote sensing. In these areas he has published more than 20 technical articles.



**Manuel A. Abreu** graduated in physics from Nova University of Lisbon in 1989, and received his PhD degree in physics engineering from the Technical University of Lisbon in 1996. He has been with INETI since 1987, working on various projects in the areas of optics, optoelectronics, and high-speed electronics as a research fellow. As coordinator of the Laser and Engineering Systems Group of the optoelectronics department, he is presently involved in a project concerning the development of eye-safe optical laser radar, among several other projects related with lasers and laser processing systems. He is author of more than 15 technical papers presented in international conferences or published in peer-reviewed journals.



**F. Carvalho Rodrigues** received his PhD in electrotechnical engineering from the University of Liverpool. Currently he is Science Administrator at NATO Headquarters, Brussels, on leave from the Universidade Independente, Faculdade de Ciências de Engenharia, Lisbon, Portugal, where he is Pro-Rector for industrial research, Professor, and Director of the Faculty of Engineering Science. Since 2001, he has been the Scientific Coordinator of UNIDCOM.

From 1985 to 1996, he was a professor at the Instituto Superior Técnico (Technical University of Lisbon). From 1980 to 1987, he was a director of the basic training course in ophthalmic optics for the National Opticians Association, and founder and first director of the Portuguese School of Optics and Optometry. As a specialist in the theory of information, optics, and optoelectronics he has published worldwide more than 200 papers. He has four books published in Portugal, one in the Russian Federation, and has contributed to another in the United States.